Age-dependent changes of nuclear morphology are uncoupled from longevity in *Caenorhabditis elegans* IGF/insulin receptor *daf-2* mutants

Mercedes M. Pérez-Jiménez, María Jesús Rodríguez-Palero, Eduardo Ródenas, Peter Askjaer†, Manuel J. Muñoz†

Centro Andaluz de Biología del Desarrollo (CABD), Consejo Superior de Investigaciones Científicas – Universidad Pablo de Olavide – Junta de Andalucía, Carretera de Utrera, km1, Seville 41013, Spain

† Corresponding authors: P Askjaer, Tel +34 954 348 396; Fax +34 954 349 376; e-mail pask@upo.es or MJ Muñoz, Tel +34 954 349 387; Fax +34 954 349 376; e-mail mmunrui@upo.es

Running title: Nuclear morphology changes during aging

Abstract

Nuclear envelope (NE) architecture and aging have been associated since the discovery that certain human progeria diseases are due to perturbations in processing of lamin A protein, generating alterations in NE morphology. However, whether changes in the NE are a causal effect of normal and premature aging is still controversial. *Caenorhabditis elegans* is a model organism where observations supporting both, dependent and independent roles of nuclear architecture in the aging process, have been reported. Using this model organism, we found that the long-lived *glp-1* mutant and dietary restriction delayed age-associated nuclear morphology changes. In addition, we observed that the long-lived mutant of the insulin/IGF receptor *daf-2* delayed the age-dependent changes of nuclear architecture at 25ºC, as previously described. However, when *daf-2* animals were incubated at 20ºC they remained long-lived, but nuclear appearance changed at similar rate as in the wild type. This supports the idea that both phenotypes, longevity and maintenance of nuclear architecture are tightly associated but can be separated and argues that nuclear morphology deterioration is not a cause of the natural aging process.

Keywords: Aging; Dietary Restriction; *daf-2*; IGF Receptor; Nuclear lamina; Progeria

1. Introduction

Three genes involved in nuclear envelope (NE) architecture have been directly related to human progeroid syndromes: *LMNA*, which encodes lamins A and C that together with B-type lamins constitute the nuclear lamina (Eriksson et al. 2003), *ZMPSTE24*, also known as *FACE*, which encodes a metalloprotease involved in prelamin A maturation (Varela et al. 2005), and *BANF1* (barrier to autointegration factor 1), which

is involved in nuclear assembly (Puente et al. 2011). Mutations in any of these genes cause a variety of diseases known as laminopathies (Worman 2012). Premature aging, such as Hutchinson-Gilford progeria syndrome (HGPS), constitutes one class of laminopathies and are accompanied by profound changes in NE architecture. Mutations affecting *LMNA* and *FACE* disrupt the processing of lamin A and lead to accumulation of immature farnesylated prelamin A protein, which is thought to be responsible for the changes in nuclear morphology and the onset of premature aging (Reddy and Comai 2012). In support of this, treatment with farnesyl transferase inhibitors reverses nuclear morphology defects in cultured progeria cells (Yang et al. 2005) and has recently been reported to improve the physiology of HGPS patients (Gordon et al. 2012). Alterations in NE architecture is not specific to progeria but have been observed also in cultured cells from donors of advanced age as well as in senescent cultured human cells and accumulation of farnesylated prelamin A has been proposed to play a role in the physiologic aging process (Raz et al. 2008; Righolt et al. 2011; Scaffidi and Misteli 2006). While numerous experiments strongly suggest a correlation between NE structure and aging, it is less clear which mechanisms are involved and whether NE deterioration plays a deterministic role in aging. It has been postulated that disruptions of NE architecture increase nuclear fragility. This would have consequences primarily on tissues where cells and nuclei face physical tension, such as muscles, which indeed are affected in several laminopathies (Worman 2012). Alternatively, it has been proposed that farnesylated prelamin A through interactions with chromatin-binding proteins could affect transcription in a way that triggers the aging process (Reddy and Comai 2012).

Caenorhabditis elegans is a very powerful animal model to study the aging process (Kenyon 2010). Similarly to what has been described for cultured human cells,

profound changes in NE morphology have been observed in aged nematodes (Haithcock et al. 2005). Many mutations have been identified in *C. elegans* that delay aging, in particular by impinging on the insulin/IGF homologue pathway (Kenyon 2010). Interestingly, mutations that reduce insulin/IGF signalling, in addition to increase longevity, delay the age-associated nuclear morphology changes (Haithcock et al. 2005), suggesting a correlation between NE morphology and the normal process of aging also in this organism. However, inhibition of farnesylation through drug treatment or by depletion of the polyprenyl synthetase FDPS-1, a key enzyme in the production of the farnesyl isoprenoid, slows down age-related deterioration of nuclear morphology in *C. elegans* without affecting longevity, suggesting the two phenotypes may be independent (Bar and Gruenbaum 2010; Bar et al. 2009). While experiments aiming to prevent farnesylation are very valuable to understand the processing of lamin proteins, they have the intrinsic complication that numerous other proteins, which are normally farnesylated, may also be affected and thus, may influence a complex trait phenotype as longevity (Ahearn et al. 2012).

To provide further insight into the emerging relationship between aging and NE structure, we have studied the nuclear architecture of long-lived animals affected in different lifespan pathways. Our data support the hypothesis that nuclear deterioration is delayed in animals with increased lifespan, but, importantly, not in all genetic backgrounds.

2. Material and Methods

2.1 C. elegans strains and culture conditions

Strain PD4810 *ccIs4810*[pJKL380.4 P_{lmn-1}*::lmn-1::gfp::lmn-1 3'UTR* + pMH86 *dpy-20(+)*] X, which expresses LMN-1::GFP in all somatic tissues, was provided by Dr. Yosef Gruenbaum (Haithcock et al. 2005). Strains TJ401 *age-1(hx546) fer-15(b26)* II, CB1370 *daf-2(e1370)* III, DR1572 *daf-2(e1368)* III, CF1038 *daf-16(mu86)* I and CB4037 *glp-1(e2141ts)* III were obtained from the *Caenorhabditis* Genetic Center (CGC) and crossed with PD4810. All strains were cultured using standard *C. elegans* methods (Stiernagle 2006). Synchronized populations were obtained by hypochlorite treatment to release embryos. Next generation, when reaching L4 stage, animals were transfered to NGM plates with 200 µM 5-fluoro 2-deoxyuridine (FUDR) to prevent progeny from hatching. Sterility in *glp-1(e2141)* was induced by incubating worms at 25ºC during larval development after which animals were moved to 20ºC. Dietary restriction (DR) experiments were performed as described (Chen et al. 2009). An *E. coli* OP50 bacterial suspension of 10^9 cfu/mL (DR) or 10^{11} cfu/mL (control) was used to seed agar plates without peptone and containing carbenicilin (50 µg/ml) to prevent bacteria growth.

2.2 Nuclear morphology assays

Three-five animals of each genotype were observed every 1-4 days. Except for t=0 (larval stage L4) data were binned into 2 days windows and for each time point numerous nuclei were observed (mean±s.e.m.: 117±4). Nuclear morphology was classified into three groups (I-III) as described in Results. Consistency in classification was achieved by different researchers scoring the same nuclei followed by blind consensus discussion. Rate of nuclear morphology deterioration, which we defined as

decreased frequency of class I and II nuclei, was determined by linear regression analysis of observations from t=0 to the last time point at which both control and mutant animals were alive.

Subtle changes in environmental conditions (laboratory room temperature, culture media batch-to-batch variation, etc.) can induce fluctuations in the rate of nuclear morphology alteration between experiments (see Supplementary Fig. S1). Within each experiment, control and mutant animals were therefore always cultured and assayed in parallel from start of the experiment to decease of the sample population. All experiments were performed at least twice.

2.3 Microscopy

Nuclear morphology was observed by anaesthetizing animals in 10 mM levamisole and mounting them on thin 3% agarose pads. For each animal, three confocal images of fluorescent LMN-1::GFP in hypodermal or intestinal cells were acquired on a Leica SP2 microscope using a 63× objective.

2.4 Lifespan assay

Lifespan assays were performed as described (Haithcock et al. 2005). Animals were examined every 2-3 days and transferred to fresh plates once a week. Animals that crawled off the plate or displayed extruded internal organs were considered censored. Animals were considered dead when they failed to respond to touch. Kaplan-Meir curves were analyzed with GraphPad Prism 5.0 Software. All experiments were performed at least twice.

3. Results

In order to study the correlation between delay in the aging process and nuclear architecture deterioration, we examined nuclear morphology at various time points in wild type and long-lived animals affected in different longevity pathways. To visualize NE structure, we used transgenic strains that carry a translational fusion of GFP with *lmn-1*, which encodes the single *C. elegans* lamin protein (Haithcock et al. 2005). We focused primarily on hypodermal nuclei, since they are easily observed by live microscopy, and classified nuclear morphology in three different categories as described in (Haithcock et al. 2005). Briefly, class I nuclei have uniform LMN-1::GFP staining along smooth NEs whereas class II nuclei show enhanced intranuclear LMN-1::GFP signal and mildly lobulated NEs with no or few bright GFP foci. Class III are characterized by highly irregular nuclear shape and accumulation of LMN-1::GFP in bright foci and reduced peripheral GFP signal (Fig 1a). NE morphology was observed each 1-4 days and the percentages of nuclei belonging to each of the classes were calculated.

Previously, experiments performed at 25ºC demonstrated that mutants affected in the insulin/IGF signalling pathway, *daf-2(e1370)* and *age-1(hx546)*, show a delay in NE morphology changes (Haithcock et al. 2005). We confirmed that deterioration of nuclear morphology is delayed in the long-lived *daf-2(e1370)* at 25ºC (Fig. 1b-d). In L4s (t=0d) class I and II nuclei were equally frequent for both control and *daf-2* (Fig. 1b). However, class III nuclei accumulated significantly slower in *daf-2* mutants, reaching 31% at day 12 of adulthood, in comparison to 48% of hypodermal nuclei in control animals (the last time point at which control animals were still alive; $P<0.01$ for t=8, t=10 and $P<0.05$ for t=12 by Chi-square test). Linear regression analysis revealed that the rate of class III appearance was reduced by 50% in *daf-2* mutants compared to

control animals ($0.018\times day^{-1}$ versus $0.037\times day^{-1}$; Fig. 1c). During the following days, the frequency of category III nuclei increased to 55% in *daf-2* mutants, and, interestingly, remained constant for the next 18 days. We also tested the long-lived mutant *glp-1(e2141ts)*, which lacks germ-line cells and acts independently of the insulin/IGF receptor (Arantes-Oliveira et al. 2002). Similarly to *daf-2* mutants, we observed a 46% delay in nuclear morphology deterioration in *glp-1* mutants ($0.0066\times day^{-1}$ versus $0.012\times day^{-1}$; Fig. 2a-b), which indicates a correlation between aging and nuclear architecture also in this longevity pathway. As a different means to increase lifespan we subjected wild type animals to dietary restriction by serial dilution of bacteria ((Chen et al. 2009); Fig. 3c). This intervention also delayed deterioration of nuclear organization by 35% ($0.022\times day^{-1}$ in dietary restricted animals versus $0.033\times day^{-1}$ in control animals; Fig. 3a-b).

Surprisingly, the delay in nuclear morphology alteration was not observed when *daf-2(e1370)* mutants were incubated at 20ºC where class III frequency increased similarly than in the wild type in five independent assays with a mean rate of $0.013\times day^{-1}$ for *daf-2(e1370)* and $0.014\times day^{-1}$ for wild-type (Fig. 4a-b represent the data from two experiments where *daf-2(e1368)* and *daf-16(mu86)* were analysed in parallel; Supplementary Fig. S1 represents the data from three additional experiments), despite animals also being long-lived at this temperature ((Gems et al. 1998); Fig. 4e). Consistently with this observation, nuclear deterioration was neither delayed in another *daf-2* allele, *e1368*, at 20ºC, with a mean rate of class III appearance of $0.019\times day^{-1}$. At days 14, 20 and 22, *daf-2(e1368)* mutants showed even a statistically significant higher frequency of class III nuclei (Fig. 4a-b). We confirmed that *daf-2(e1368)* is also long-lived at 20ºC (Fig. 4e). Together, these data strongly indicate a dissociation of increased longevity from delay of changes in nuclear morphology in two different *daf-2* alleles.

This is not due to a general effect on NE dynamics by reduction of the temperature because *age-1(hx546)*, which belongs to the same genetic pathway as *daf-2*, delays by 49% NE morphology changes associated with aging at 20ºC ($0.015 \times day^{-1}$ versus $0.030 \times day^{-1}$; Fig. 5a-b), similarly to the result described at 25ºC (Haithcock et al. 2005). We have also measured the rate of nuclear deterioration in a short-lived *daf-16* deletion mutant incubated at 20ºC. *daf-16* is the downstream FOXO transcription factor of the insulin/IGF pathway, that when mutated suppresses the increased longevity of *daf-2* mutants ((Lin et al. 1997; Ogg et al. 1997); Fig. 4e). We observed that NE morphology was altered at identical rate in *daf-16* single and *daf-16; daf-2* double mutants at 20ºC (both show a rate of $0.016 \times day^{-1}$) and similarly to control animals ($0.014 \times day^{-1}$; Fig. 4c-d). This result suggests that the short lifespan of *daf-16* mutants is not coupled to accelerated nuclear deterioration at 20ºC.

4. Discussion

Whether changes in nuclear morphology contribute to the aging phenotype in Hutchinson-Gilford progeria syndrome (HPGS) or play a role in natural aging is still controversial. Correlations between the two phenomena have been reported both in HGPS and during the normal process of aging. The observation that in *C. elegans*, longevity induced by mutations in the insulin/IGF pathway correlates with reduced NE deterioration rate suggests moreover a functional relation between aging and nuclear morphology (Haithcock et al. 2005). Several of our results support this hypothesis, since long-lived dietary-restricted animals, *age-1(hx546)* and *glp-1(e2141ts)* mutants as well as *daf-2(e1370)* at 25ºC showed a clear delay in alteration of nuclear appearance. However, the most important observation in this study was that increased longevity was uncoupled from delay in age-associated changes of NE architecture in two different *daf-2* mutants incubated at 20ºC. The finding that the correlation between both processes was temperature dependent was unique to *daf-2* mutants since *age-1* displays the correlation both at 20ºC (this study) and at 25ºC (Haithcock et al. 2005). The difference observed between *daf-2* and *age-1* mutants is intriguing because both genes belong to the same genetic pathway. However, *age-1* independent *daf-2* phenotypes have been described (Paradis et al. 1999; Wolkow et al. 2002). We therefore speculate that parallel pathways downstream of *daf-2* may have different effects on nuclear architecture maintenance at 20ºC. Identification of genes acting in these pathways is critical to address this possibility.

The fact, that two independent *daf-2* alleles behaved similarly at 20ºC and the absence of additive effects in the *daf-16; daf-2* double mutant indicate that the cause of the uncoupling between aging and nuclear deterioration is not due the presence of additional mutations carried by the *daf-2* strains but is rather a feature of the *daf-2*

alleles. In addition, we report that nuclear deterioration occurred at similar rate in wild type animals and short-lived *daf-16* mutants at 20ºC, whereas an increase in deterioration was previously observed at 25ºC for this mutant (Haithcock et al. 2005). This further enforces our observation that aging and nuclear archictecture maintenance can be genetically uncoupled.

The temperature dependent behavior of *daf-2(e1370)* and *daf-16(mu86)* is intriguing and may indicate a role of chaperones and/or heat shock proteins in the maintenance of the nuclear architecture. These protective proteins may potentially be higher expressed at 25ºC than at 20ºC and could help in the maintenance of the nuclear structure in a longevity-dependent manner. Interestingly, higher nuclear deterioration rate has been observed in the heat shock factor 1, *hsf-1* mutant at 25ºC (Haithcock et al. 2005). The expression analysis of chaperones in *daf-2* mutants and *age-1* at 20ºC and at 25ºC may help to elucidate the role of these proteins in nuclear envelope maintenance.

Nevertheless, the fact that in several genetic situations lifespan and nuclear morphology changes are uncoupled, strongly suggests that age-associated alteration of nuclear morphology is not sufficient to cause aging, although the phenomena are linked. Recently, it was reported that in *C. elegans*, pharmacological treatment that inhibits farnesylation or depletion of the polyprenyl synthetase FDPS-1, a key enzyme in the production of the farnesyl isoprenoid, reverses age-dependent nuclear morphology without affecting lifespan, thus also uncoupling the two processes (Bar and Gruenbaum 2010; Bar et al. 2009). Our results are complementary to this, where we observed long-lived animals with a wild-type rate of NE deterioration. Since inhibition of farnesylation affects not only nuclear lamina proteins but also a variety of other proteins, including key signaling molecule Ras, our results provide an important genetic verification of the possibility of uncoupling longevity from NE deterioration. These data are of special

relevance for the development of new therapies for NE-related progeria syndromes and indicate that treatments, which reverse the age-dependent nuclear morphology deterioration, may not prevent the accelerated aging process.

5. Acknowledgements

We wish to thank Y. Gruenbaum for the PD4810 strain and J. Rueda-Carrasco for technical assistance as well as M. Artal-Sanz, A.M. Brokate-Llanos and A. Miranda-Vizuete for discussion on the manuscript. This work was funded by the Autonomous Government of Andalusia (P07-CVI-02697). In addition, we wish to acknowledge Fundación Ramón Areces for a fellowship to ER. Some nematode strains used in this work were provided by the "*Caenorhabditis* Genetic Center", which is funded by the NIH National Center for Research Resources (NCRR).

6. References

Ahearn IM, Haigis K, Bar-Sagi D, Philips MR (2012) Regulating the regulator: post-translational modification of RAS. Nat Rev Mol Cell Biol 13 (1):39-51. doi:10.1038/nrm3255

Arantes-Oliveira N, Apfeld J, Dillin A, Kenyon C (2002) Regulation of life-span by germ-line stem cells in *Caenorhabditis elegans*. Science 295 (5554):502-505. doi:10.1126/science.1065768

Bar DZ, Gruenbaum Y (2010) Reversal of age-dependent nuclear morphology by inhibition of prenylation does not affect lifespan in *Caenorhabditis elegans*. Nucleus 1 (6):499-505. doi:10.4161/nucl.1.6.13223

Bar DZ, Neufeld E, Feinstein N, Gruenbaum Y (2009) Gliotoxin reverses age-dependent nuclear morphology phenotypes, ameliorates motility, but fails to affect lifespan of adult *Caenorhabditis elegans*. Cell motility and the cytoskeleton 66 (10):791-797. doi:10.1002/cm.20347

Chen D, Thomas EL, Kapahi P (2009) HIF-1 modulates dietary restriction-mediated lifespan extension via IRE-1 in *Caenorhabditis elegans*. PLoS Genet 5 (5):e1000486. doi:10.1371/journal.pgen.1000486

Eriksson M, Brown WT, Gordon LB, Glynn MW, Singer J, Scott L, Erdos MR, Robbins CM, Moses TY, Berglund P, Dutra A, Pak E, Durkin S, Csoka AB, Boehnke M, Glover TW, Collins FS (2003) Recurrent de novo point mutations in lamin A cause Hutchinson-Gilford progeria syndrome. Nature 423 (6937):293-298. doi:10.1038/nature01629

Gems D, Sutton AJ, Sundermeyer ML, Albert PS, King KV, Edgley ML, Larsen PL, Riddle DL (1998) Two pleiotropic classes of *daf-2* mutation affect larval arrest, adult behavior, reproduction and longevity in *Caenorhabditis elegans*. Genetics 150 (1):129-155

Gordon LB, Kleinman ME, Miller DT, Neuberg DS, Giobbie-Hurder A, Gerhard-Herman M, Smoot LB, Gordon CM, Cleveland R, Snyder BD, Fligor B, Bishop WR, Statkevich P, Regen A, Sonis A, Riley S, Ploski C, Correia A, Quinn N, Ullrich NJ, Nazarian A, Liang MG, Huh SY, Schwartzman A, Kieran MW (2012) Clinical trial of a farnesyltransferase inhibitor in children with Hutchinson-Gilford progeria syndrome. Proc Natl Acad Sci U S A 109 (41):16666-16671. doi:10.1073/pnas.1202529109

Haithcock E, Dayani Y, Neufeld E, Zahand AJ, Feinstein N, Mattout A, Gruenbaum Y, Liu J (2005) Age-related changes of nuclear architecture in *Caenorhabditis elegans*. Proc Natl Acad Sci U S A 102 (46):16690-16695

Kenyon CJ (2010) The genetics of ageing. Nature 464 (7288):504-512. doi:10.1038/nature08980

Lin K, Dorman JB, Rodan A, Kenyon C (1997) daf-16: An HNF-3/forkhead family member that can function to double the life-span of *Caenorhabditis elegans*. Science 278 (5341):1319-1322

Ogg S, Paradis S, Gottlieb S, Patterson GI, Lee L, Tissenbaum HA, Ruvkun G (1997) The Fork head transcription factor DAF-16 transduces insulin-like metabolic and longevity signals in *C. elegans*. Nature 389 (6654):994-999. doi:10.1038/40194

Paradis S, Ailion M, Toker A, Thomas JH, Ruvkun G (1999) A PDK1 homolog is necessary and sufficient to transduce AGE-1 PI3 kinase signals that regulate diapause in *Caenorhabditis elegans*. Genes Dev 13 (11):1438-1452

Puente XS, Quesada V, Osorio FG, Cabanillas R, Cadinanos J, Fraile JM, Ordonez GR, Puente DA, Gutierrez-Fernandez A, Fanjul-Fernandez M, Levy N, Freije JM, Lopez-Otin C (2011) Exome sequencing and functional analysis identifies BANF1 mutation as the cause of a hereditary progeroid syndrome. American journal of human genetics 88 (5):650-656. doi:10.1016/j.ajhg.2011.04.010

Raz V, Vermolen BJ, Garini Y, Onderwater JJ, Mommaas-Kienhuis MA, Koster AJ, Young IT, Tanke H, Dirks RW (2008) The nuclear lamina promotes telomere aggregation and centromere peripheral localization during senescence of human mesenchymal stem cells. J Cell Sci 121 (Pt 24):4018-4028. doi:10.1242/jcs.034876

Reddy S, Comai L (2012) Lamin A, farnesylation and aging. Exp Cell Res 318 (1):1-7. doi:10.1016/j.yexcr.2011.08.009

Righolt CH, van 't Hoff ML, Vermolen BJ, Young IT, Raz V (2011) Robust nuclear lamina-based cell classification of aging and senescent cells. Aging (Albany NY) 3 (12):1192-1201

Scaffidi P, Misteli T (2006) Lamin A-dependent nuclear defects in human aging. Science 312 (5776):1059-1063. doi:10.1126/science.1127168

Stiernagle T (2006) Maintenance of *C. elegans*. WormBook:1-11. doi:10.1895/wormbook.1.101.1

Varela I, Cadinanos J, Pendas AM, Gutierrez-Fernandez A, Folgueras AR, Sanchez LM, Zhou Z, Rodriguez FJ, Stewart CL, Vega JA, Tryggvason K, Freije JM, Lopez-Otin C (2005) Accelerated ageing in mice deficient in Zmpste24 protease is linked to p53 signalling activation. Nature 437 (7058):564-568. doi:10.1038/nature04019

Wolkow CA, Munoz MJ, Riddle DL, Ruvkun G (2002) Insulin receptor substrate and p55 orthologous adaptor proteins function in the *Caenorhabditis elegans daf-2*/insulin-like signaling pathway. J Biol Chem 277 (51):49591-49597. doi:10.1074/jbc.M207866200

Worman HJ (2012) Nuclear lamins and laminopathies. The Journal of pathology 226 (2):316-325. doi:10.1002/path.2999

Yang SH, Bergo MO, Toth JI, Qiao X, Hu Y, Sandoval S, Meta M, Bendale P, Gelb MH, Young SG, Fong LG (2005) Blocking protein farnesyltransferase improves nuclear blebbing in mouse fibroblasts with a targeted Hutchinson-Gilford progeria syndrome mutation. Proc Natl Acad Sci U S A 102 (29):10291-10296. doi:10.1073/pnas.0504641102

Figure legends

Fig. 1 Nuclear morphology deterioration is slowed down in *daf-2* mutants at 25°C. (**a**) Classification of nuclear morphology. Hypodermal nuclei of *C. elegans* expressing LMN-1::GFP were observed by confocal microscopy and grouped into three classes based on nuclear envelope morphology (see text for details). To compensate for lower LMN-1::GFP expression in younger versus older animals, images were individually adjusted for contrast and brightness. Scale bar, 10 µm. (**b**) Cumulative bar plot comparing frequencies of class I (green), class II (yellow) and class III (red) hypodermal nuclear morphology in control (pale, dotted bars) and *daf-2(e1370)* (bright, hatched bars) animals incubated at 25°C during adulthood. Asterisks indicate time points where the frequency of class III nuclei in the test population is significantly decreased relative to the control population (* $P<0.05$ and ** $P<0.01$ by Chi-square test). (**c**) Rate of class III appearance represented by decreasing frequency of class I and II nuclei. Only time points where data were available for both strains are included. Black and blue lines were generated by linear regression on control and *daf-2* data, respectively (wt correlation coefficient $R^2=0.84$; *daf-2* $R^2=0.63$). (**d**) Survival curves for wt (black) and *daf-2* (blue) illustrate that *daf-2* mutants live significantly longer than wt animals ($p<0.0001$, Mantel-Cox test). Error bars indicate standard error of the means.

Fig. 2 Genetic germ line ablation reduces nuclear morphology deterioration. (**a**) Cumulative bar plot comparing control (dotted bars) and *glp-1(e2141ts)* (hatched bars) animals raised at 25°C and incubated at 20°C during adulthood. (**b**) Linear regression analysis of control (black) and *glp-1* (blue) data (wt R^2=0.73; *glp-1* R^2=0.49). See Fig. 1 for further description.

Fig. 3 Dietary restriction reduces nuclear morphology deterioration. (**a**) Cumulative bar plot comparing control (pale, dotted bars) and dietary restricted (*DR*; bright, hatched bars) animals incubated at 25°C during adulthood. (**b**) Linear regression analysis of control (black) and *DR* (blue) data (wt R^2=0.85; *DR* R^2=0.84). (**c**) Survival curves for control (black) and *DR* (blue) animals illustrate that dietary restriction extends lifespan significantly (P<0.0001, Mantel-Cox test). Error bars indicate standard error of the means. See Fig 1 for further description.

Fig. 4 Nuclear morphology deteriorates with wild type kinetics in *daf-2* and *daf-16* mutants at 20°C. (**a**) Cumulative bar plot comparing control (pale, dotted bars), *daf-2(e1370)* (bright, hatched bars) and *daf-2(e1368)* (dark, empty bars) animals incubated at 20°C during adulthood. Hash tags indicate time points where the frequency of class III nuclei in the test population is significantly increased relative to the control population (# P<0.05 and ## P<0.01 by Chi-square test). (**b**) Linear regression analysis of control (black), *daf-2(e1370)* (blue), and *daf-2(e1368)* (green) data (wt R^2=0.89; *daf-2(e1370)* R^2=0.78; *daf-2(e1368)* R^2=0.89). (**c**) Cumulative bar plot comparing control (pale, dotted bars; same dataset as in (**a**)), *daf-16(mu86)* (bright, hatched bars) and *daf-16(mu86); daf-2(e1370)* (dark, empty bars) animals incubated at 20°C during

adulthood. (**d**) Linear regression analysis of control (black), *daf-16(mu86)* (blue), *daf-16(mu86)*; *daf-2(e1370)* (green) data (wt R^2=0.89; *daf-16(mu86)* R^2=0.76; *daf-16(mu86)*; *daf-2(e1370)* R^2=0.84). (**e**) Survival curves for wt (black), *daf-2(e1370)* (dark blue), *daf-2(e1368)* (light blue), *daf-16(mu86)* (light green) and *daf-16; daf-2(e1370)* (dark green) illustrate that *daf-2* mutants live significantly longer than wt animals, whereas *daf-16* single and *daf-16; daf-2* double mutants live significantly shorter (P<0.0001 for all mutants compared to wt, Mantel-Cox test). Error bars indicate standard error of the means. See Fig. 1 for further description

Fig. 5 Nuclear envelope alterations are delayed in *age-1* mutants (**a**) Cumulative bar plot comparing control (pale, dotted bars) and *age-1(hx546)* (bright, hatched bars) animals incubated at 20°C. (**b**) Linear regression analysis of control (blue) and *age-1* (red) data (wt R^2=0.93; *age-1* R^2=0.83). See Fig. 1 for further description.

Figure1
Click here to download Figure: Figure1.eps

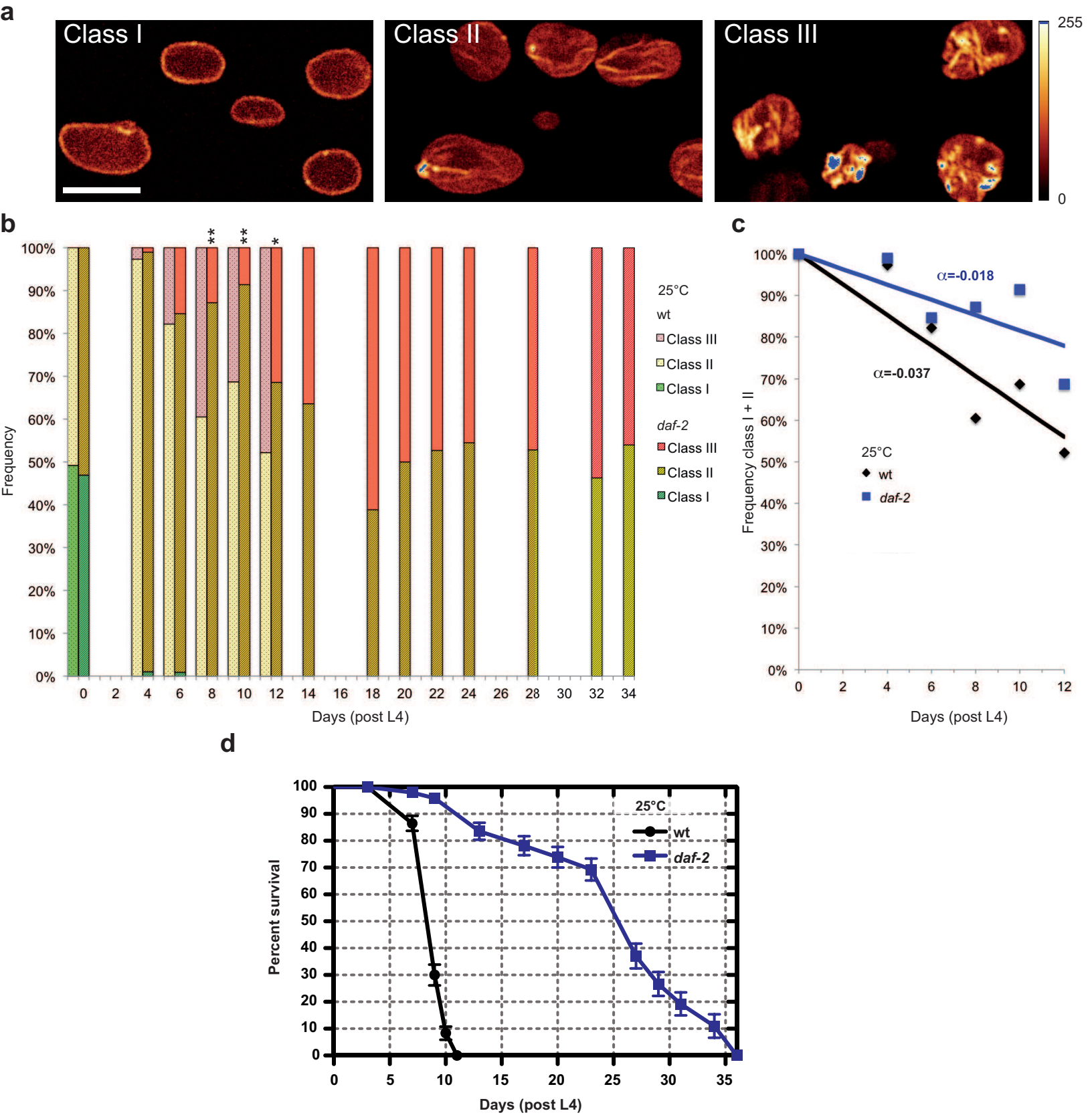

Figure2
Click here to download Figure: Figure2.eps

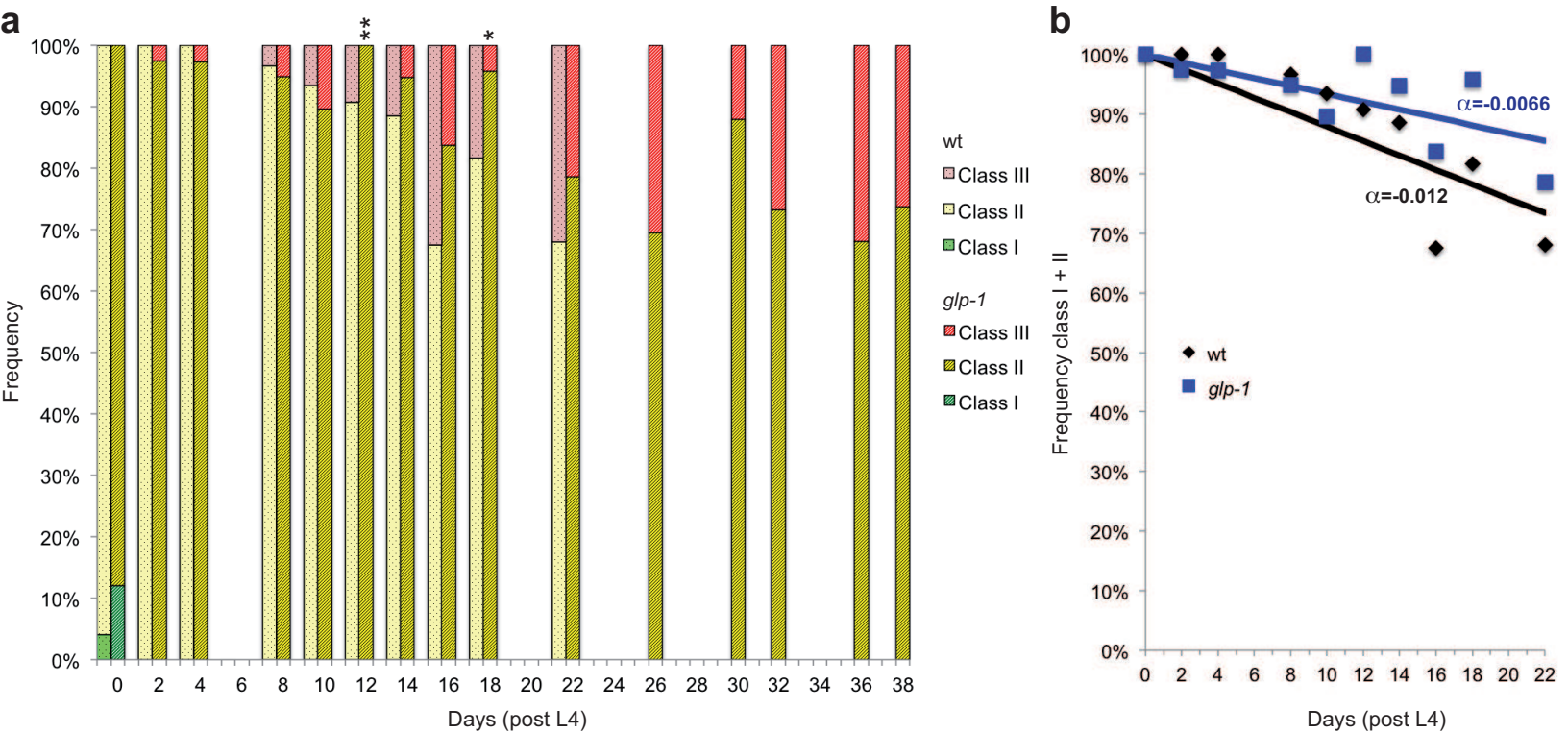

Figure3
Click here to download Figure: Figure3.eps

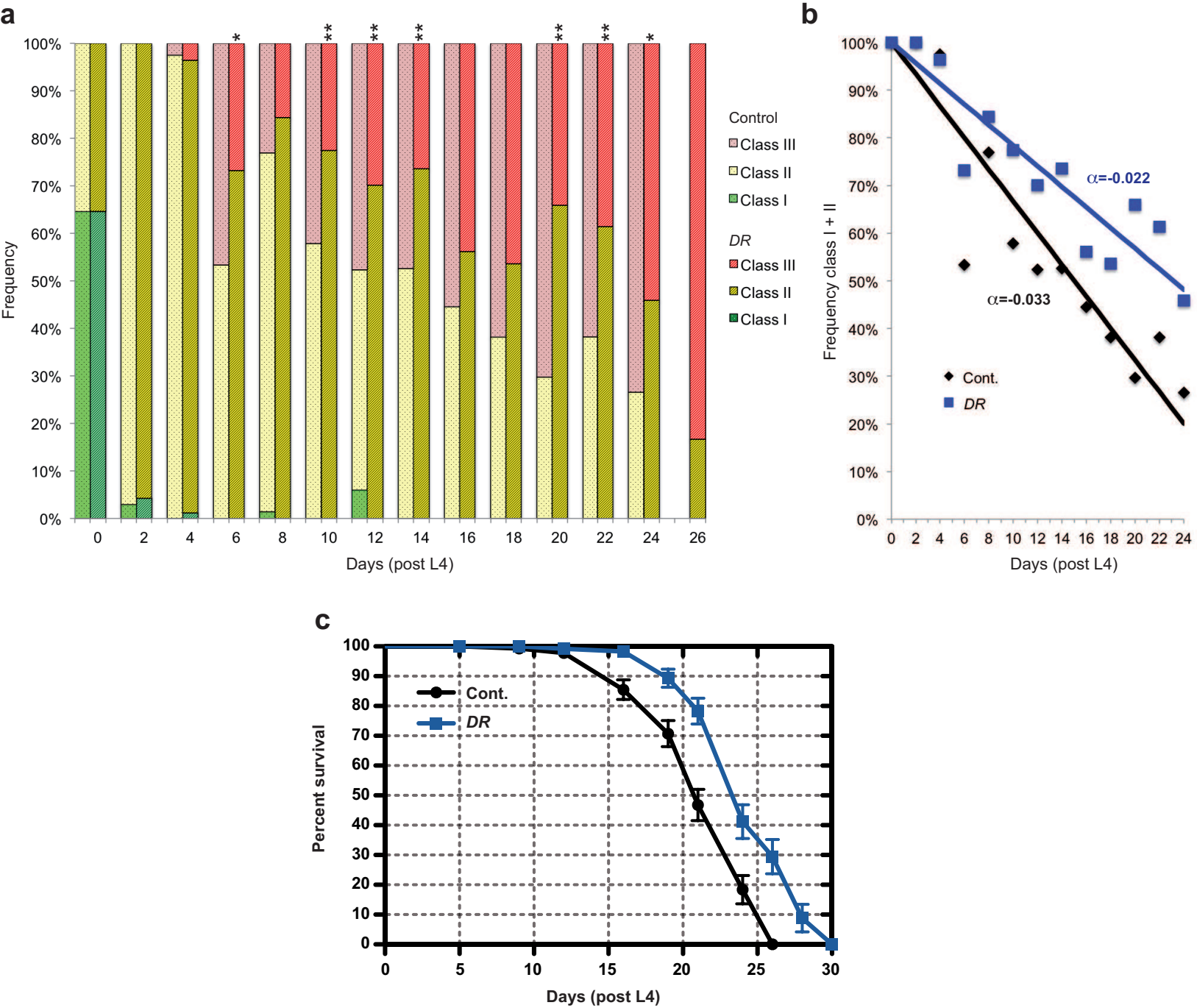

Figure4

Click here to download Figure: Figure4.eps

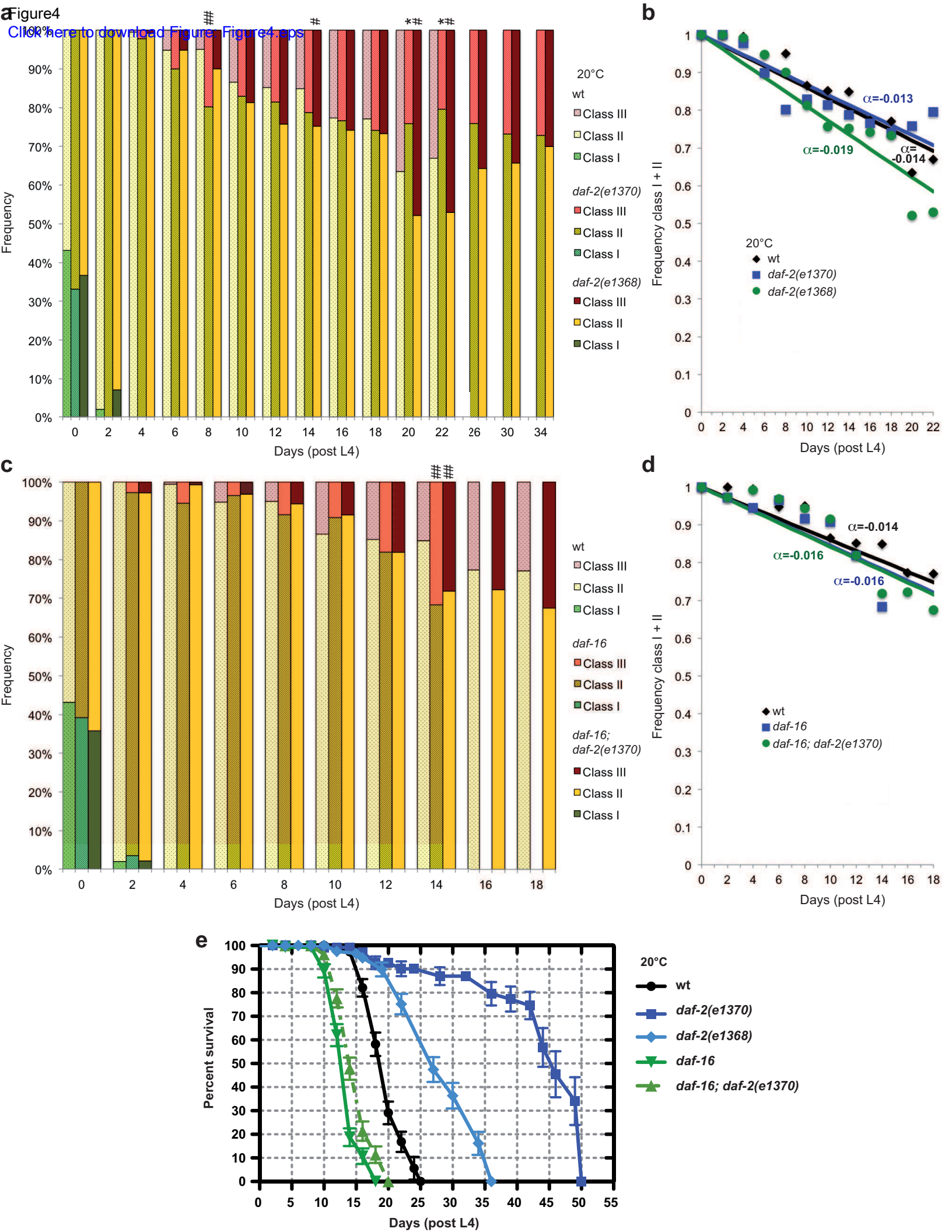

Figure5
Click here to download Figure: Figure5.eps

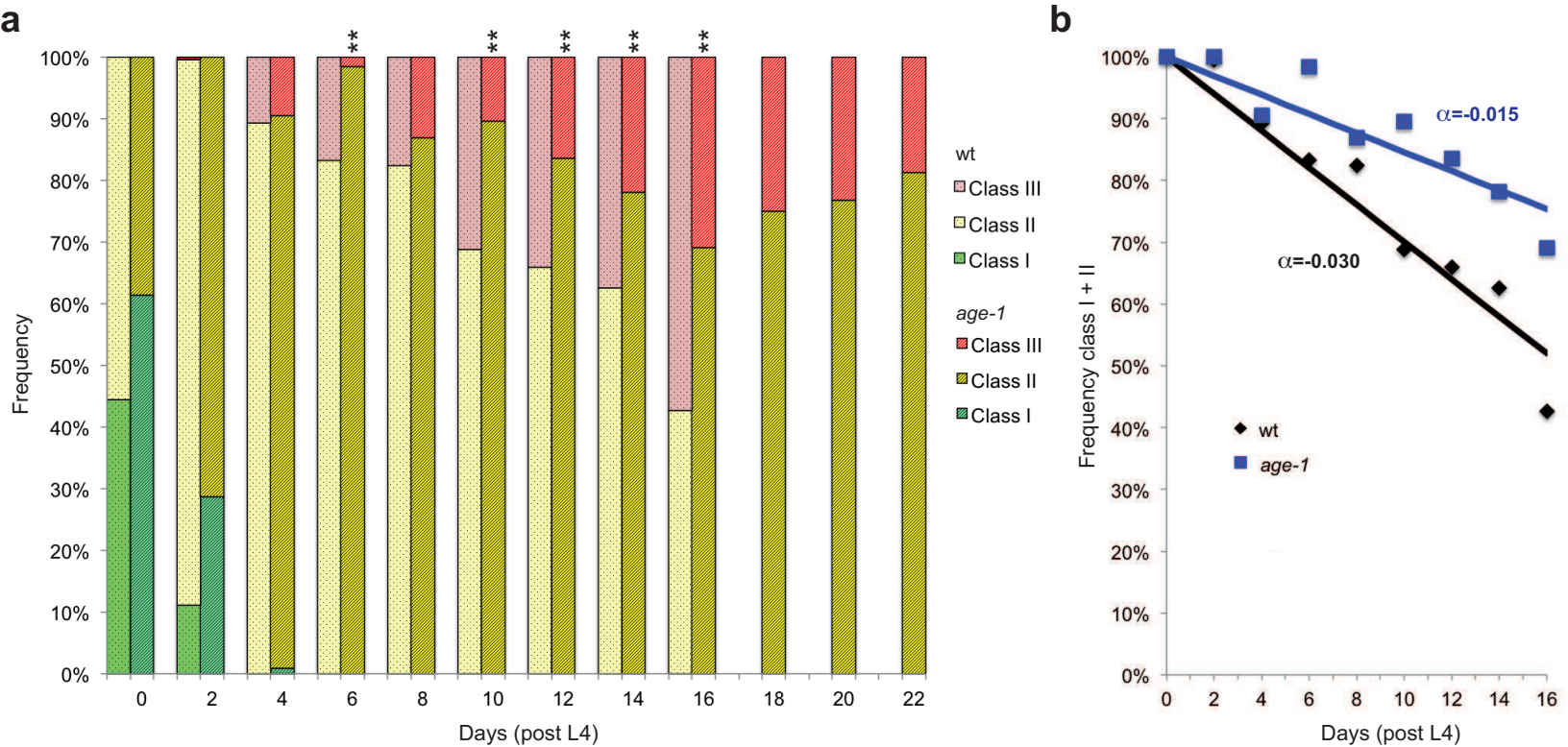

Figure1S

Click here to download Supplementary Material: FigureS1.tif

Click here to view linked References